Supplementary information for "**Thermal liability of hyaloclastite in the Krafla geothermal reservoir, Iceland: the impact of phyllosilicates on permeability and rock strength"**

Josh Weaver[1*], Guðjón H. Eggertsson[1], James E.P. Utley[1], Paul A. Wallace[1], Anthony Lamur[1], Jackie E. Kendrick[1], Hugh Tuffen[2], Sigurður H. Markússon[3], Yan Lavallée[1].

[1]Department of Earth, Ocean and Ecological Sciences, University of Liverpool, 4 Brownlow Street, L69 3GP, Liverpool, UK

[2]Lancaster Environment Centre, Lancaster University, LA1 4YQ, Lancaster, UK

[3]Landsvirkjun, Háaleitisbraut 68, 110 Reykjavík, Iceland

*j.weaver@liverpool.ac.uk

This file contains the supplementary information used for analysis in the main paper.

1. Sample Physical and Mechanical Data

Table S1. A summary of water permeability values at a range of confining pressures.

Sample	Confining pressure	K	Porosity reduction
	(MPa)	(m^2)	(%)
HYA_0m_002 130°C	3.73	8.05E-14	n/a
	7.95	7.51E-14	0.32
	12.53	6.46E-14	0.83
	16.96	4.87E-14	1.27
	23.75	2.18E-15	2.3
	28.8	1.13E-15	3.44
HYA_0m_006 185°C	3.55	4.68E-14	n/a
	9.04	5.58E-14	0.41
	13.96	7.18E-14	1.09
	18.91	4.96E-14	1.86
	23.84	2.25E-14	2.82
	29.04	8.13E-15	4.04
HYA_0m_008 185°C	3.94	7.87E-14	n/a
	8.78	7.15E-14	0.61
	13.83	6.28E-14	1.61
	18.78	5.07E-14	2.58
	23.67	3.65E-14	3.63
	27.9	2.14E-14	4.7
HYA_0m_015 Untreated	3.55	1.56E-14	n/a
	8.65	1.85E-14	0.26

	13.6	1.68E-14	0.63
	18.65	1.63E-14	1.12
	23.7	1.26E-14	1.98
	28.65	4.37E-15	3.36
HYA_0m_020 Untreated	3.58	5.48E-16	n/a
	8.53	4.42E-16	0.31
	13.61	3.98E-16	0.75
	18.51	7.72E-16	1.27
	23.56	2.67E-16	2.09
	28.21	8.93E-16	3.27
HYA_0m_021 130°C	3.89	1.63E-14	n/a
	8.84	1.61E-14	0.56
	13.54	1.56E-14	1.37
	18.5	1.47E-14	2.22
	23.46	1.24E-14	3.37
	28.4	3.59E-15	4.89
HYA_0m_035 600°C	3.27	2.28E-15	n/a
	8.85	5.20E-15	0.83
	13.89	6.06E-15	2.27
	19.28	6.58E-15	3.56
	23.97	7.01E-15	4.67
	28.36	6.00E-15	5.57
HYA_0m_068 400°C	3.71	5.77E-15	n/a
	8.58	4.66E-15	0.74
	13.78	1.28E-14	2.01
	18.75	1.78E-14	3.15
	23.45	1.53E-14	3.7
	28.59	1.31E-14	4.39
HYA_0m_072 600°C	3.78	2.24E-13	n/a
	8.89	1.59E-13	0.8
	13.7	1.37E-13	2.2
	18.98	1.08E-13	3.48
	23.7	1.04E-13	4.72
	28.79	8.21E-14	5.84
HYA_0m_076 400°C	3.46	1.10E-13	n/a
	8.82	8.96E-14	0.83
	13.78	8.01E-14	2.27
	18.35	6.93E-14	3.56
	23.47	5.82E-14	4.67
	28.51	4.78E-14	5.57

1 Table S2. A summary of all porosity, gas permeability, compressive strength and Young's Modulus values for as-collected and thermally treated cores.

As-collected					Post-thermal treatment						
Sample	Density	Porosity	Gas K	TT	Density	Mass reduction	Porosity	Gas K	UCS	TXL	Young's Modulus
	(g/cm^3)	(%)	(m^2)	(°C)	(g/cm^3)	(g)	(%)	(m^2)	(MPa)	(MPa)	(GPa)
HYA_0m_001	2.5084	37.17	1.81E-13	n/a	n/a	n/a	n/a	n/a	n/a	n/a	n/a
HYA_0m_002	2.5016	37.58	1.33E-13	130	2.5876	1.94	40.7	1.65E-13	n/a	n/a	n/a
HYA_0m_003	2.5383	39.99	2.95E-13	130	2.6197	1.51	42.1	3.66E-13	n/a	n/a	n/a
HYA_0m_004	2.5397	38.4	2.18E-13	130	2.628	1.65	41.5	2.66E-13	n/a	n/a	n/a
HYA_0m_005	2.5405	38.24	2.89E-13	130	2.6247	1.5	42.4	3.63E-13	n/a	n/a	n/a
HYA_0m_006	2.5527	36.75	1.53E-13	185	2.6204	1.02	42.2	2.30E-13	n/a	n/a	n/a
HYA_0m_007	2.5015	34.38	7.21E-14	185	2.6145	2.06	40.2	1.24E-13	n/a	n/a	n/a
HYA_0m_008	2.506	36.08	1.34E-13	185	2.6222	1.95	41.8	2.23E-13	n/a	n/a	n/a
HYA_0m_009	2.5515	39.06	1.87E-13	185	2.6173	0.94	42	2.47E-13	n/a	n/a	n/a
HYA_0m_010	2.5691	40.29	2.72E-13	n/a	n/a	n/a	n/a	n/a	n/a	n/a	n/a
HYA_0m_011	2.5496	38.48	2.76E-13	n/a	n/a	n/a	n/a	n/a	n/a	n/a	n/a
HYA_0m_012	2.5719	40.93	3.20E-13	130	2.6214	0.76	43.1	3.71E-13	8.8	n/a	1.58
HYA_0m_013	2.5219	38.7	2.14E-13	n/a	n/a	n/a	n/a	n/a	n/a	n/a	n/a
HYA_0m_014	2.5396	36.75	2.45E-13	n/a	n/a	n/a	n/a	n/a	n/a	n/a	n/a
HYA_0m_015	2.4945	36.76	1.50E-13	n/a	n/a	n/a	n/a	n/a	n/a	n/a	n/a
HYA_0m_016	2.5639	37.69	3.69E-13	n/a	n/a	n/a	n/a	n/a	n/a	n/a	n/a
HYA_0m_017	2.5818	38.33	4.12E-13	n/a	n/a	n/a	n/a	n/a	n/a	n/a	n/a
HYA_0m_018	2.5358	38.24	2.61E-13	185	2.6452	1.71	43.3	3.68E-13	n/a	n/a	n/a
HYA_0m_019	2.5099	37.62	1.31E-13	185	2.6298	2.04	43.5	2.14E-13	n/a	n/a	n/a
HYA_0m_020	2.5017	36.65	1.47E-13	n/a	n/a	n/a	n/a	n/a	n/a	n/a	n/a

HYA_0m_021	2.5153	37.65	1.85E-13	130	2.6033	1.62	42.1	2.48E-13	n/a	n/a	n/a
HYA_0m_022	2.5067	38.29	1.86E-13	n/a	n/a	n/a	n/a	n/a	n/a	n/a	n/a
HYA_0m_023	2.5323	36.14	1.81E-13	185	2.6433	1.88	41.5	2.77E-13	n/a	n/a	n/a
HYA_0m_024	2.5975	41.82	3.72E-13	n/a	n/a	n/a	n/a	n/a	8	n/a	1.15
HYA_0m_025	2.5596	39.86	2.42E-13	185	2.6195	0.79	42.4	3.02E-13	92	n/a	0.95
HYA_0m_026	2.5767	39.67	2.21E-13	130	2.612	0.51	41.2	2.54E-13	11.5	n/a	1.91
HYA_0m_027	2.5568	40.45	1.91E-13	130	2.5925	0.45	42.1	2.21E-13	8.7	n/a	1
HYA_0m_028	2.5686	41.75	2.41E-13	185	2.6314	0.74	44.2	3.07E-13	6.3	n/a	0.66
HYA_0m_029	2.5631	39.98	1.98E-13	n/a	n/a	n/a	n/a	n/a	10.1	n/a	1.43
HYA_0m_030	2.5592	41.31	2.03E-13	n/a	n/a	n/a	n/a	n/a	8.3	n/a	1.18
HYA_0m_031	2.5531	39.84	1.75E-13	130	2.5938	0.54	41.6	2.03E-13	8.4	n/a	1.3
HYA_0m_032	2.5471	40.24	1.30E-13	185	2.6178	0.86	43.1	1.74E-13	10.5	n/a	1.41
HYA_0m_033	2.6043	40.8	4.13E-13	185	2.6558	0.7	43	4.90E-13	7	n/a	0.85
HYA_0m_034	2.5514	44.13	2.50E-13	600	2.7653	2.77	45.9	5.90E-13	6.6	n/a	0.73
HYA_0m_035	2.5036	37.96	1.70E-13	600	2.7355	3.58	47.9	5.46E-13	n/a	n/a	n/a
HYA_0m_036	2.5119	41.36	1.79E-13	600	2.7273	3.02	50.3	5.56E-13	4.2	n/a	0.49
HYA_0m_037	2.5027	37.66	2.08E-13	600	2.7279	2.74	47.1	5.55E-13	n/a	n/a	n/a
HYA_0m_038	2.527	37.89	2.17E-13	600	2.7489	2.92	47	5.68E-13	n/a	n/a	n/a
HYA_0m_039	2.5107	39.42	1.94E-13	600	2.7325	3.21	48.7	5.86E-13	5.3	n/a	0.47
HYA_0m_040	2.4976	35.7	1.73E-13	130	2.5302	0.38	39	2.13E-13	n/a	n/a	n/a
HYA_0m_041	2.5636	37.66	3.60E-13	600	2.7633	2.64	46	7.04E-13	n/a	23.1	0.56
HYA_0m_042	2.5348	40.85	2.12E-13	185	2.6498	0.61	44.3	n/a	n/a	23.8	1.79
HYA_0m_043	2.5488	40.33	2.23E-13	185	2.62	1.16	43.7	n/a	n/a	26.3	1.38
HYA_0m_044	2.5556	40.23	2.29E-13	130	2.5878	0.42	41.6	n/a	n/a	27.7	2.51
HYA_0m_045	2.5548	40.76	2.51E-13	n/a	n/a	n/a	n/a	n/a	n/a	n/a	n/a
HYA_0m_046	2.5687	40.59	2.81E-13	n/a	n/a	n/a	n/a	n/a	n/a	n/a	n/a
HYA_0m_047	2.5582	39.91	2.60E-13	n/a	n/a	n/a	n/a	n/a	n/a	29.5	3.44
HYA_0m_048	2.5523	40.37	2.08E-13	n/a	n/a	n/a	n/a	n/a	n/a	n/a	n/a

HYA_0m_049	2.5345	38.59	1.44E-13	n/a	n/a	n/a	n/a	n/a	n/a	n/a	n/a
HYA_0m_050	2.5426	39.04	2.39E-13	n/a	n/a	n/a	n/a	n/a	n/a	n/a	n/a
HYA_0m_051	2.5562	39.35	1.69E-13	n/a	n/a	n/a	n/a	n/a	n/a	n/a	n/a
HYA_0m_052	2.532	39.92	1.47E-13	n/a	n/a	n/a	n/a	n/a	n/a	n/a	n/a
HYA_0m_053	2.5858	40.02	3.35E-13	400	2.7271	1.9	45.8	5.47E-13	n/a	n/a	n/a
HYA_0m_054	2.5386	38.23	2.11E-13	400	2.6862	1.99	44.2	3.61E-13	n/a	26.3	1.33
HYA_0m_055	2.6033	40.35	4.80E-13	400	2.7385	1.84	45.8	7.53E-13	n/a	n/a	n/a
HYA_0m_056	2.5337	39.83	1.86E-13	600	2.7103	2.3	47	4.50E-13	n/a	24.1	0.68
HYA_0m_057	2.5467	40.02	2.39E-13	400	2.6791	1.84	45.7	4.27E-13	6.8	n/a	1.27
HYA_0m_058	2.5504	39.76	2.54E-13	400	2.685	1.79	45.5	4.33E-13	n/a	n/a	n/a
HYA_0m_059	2.5885	38.33	3.54E-13	400	2.7295	1.82	44.2	5.69E-13	6.3	n/a	1.32
HYA_0m_060	2.543	41.08	2.11E-13	400	2.6927	1.85	47.1	4.01E-13	n/a	n/a	n/a
HYA_0m_061	2.5482	40.6	2.14E-13	400	2.6909	1.91	46.6	4.13E-13	n/a	n/a	n/a
HYA_0m_062	2.4618	36.8	n/a	n/a	n/a	n/a	n/a	n/a	n/a	n/a	n/a
HYA_0m_063	2.4676	37.79	n/a	n/a	n/a	n/a	n/a	n/a	n/a	n/a	n/a
HYA_0m_064	2.4674	36.81	n/a	n/a	n/a	n/a	n/a	n/a	n/a	n/a	n/a
HYA_0m_065	2.5072	39.93	n/a	n/a	n/a	n/a	n/a	n/a	n/a	n/a	n/a
HYA_0m_066	2.5087	36.96	n/a	n/a	n/a	n/a	n/a	n/a	n/a	n/a	n/a
HYA_0m_067	2.5482	39.29	1.82E-13	400	2.6286	0.9	42.5	3.10E-13	n/a	n/a	n/a
HYA_0m_068	2.5449	38.61	1.56E-13	400	2.6479	1.1	42.6	2.90E-13	n/a	n/a	n/a
HYA_0m_069	2.5515	39.27	1.82E-13	n/a	n/a	n/a	n/a	n/a	n/a	n/a	n/a
HYA_0m_070	2.5497	38.46	2.51E-13	n/a	n/a	n/a	n/a	n/a	n/a	31	2.17
HYA_0m_071	2.5376	39.01	1.97E-13	130	2.5678	0.61	40.6	2.29E-13	n/a	29.6	1.52
HYA_0m_072	2.5956	38.86	3.96E-13	600	2.7501	1.91	45.1	7.42E-13	n/a	n/a	n/a
HYA_0m_073	2.5492	40	2.12E-13	400	2.6811	1.89	45.6	3.82E-13	n/a	24.7	1.1
HYA_0m_074	2.5405	38.77	3.45E-13	n/a	n/a	n/a	n/a	n/a	n/a	n/a	n/a
HYA_0m_075	2.536	40.02	2.11E-13	400	2.6878	2.32	46.5	4.18E-13	5.9	n/a	0.8
HYA_0m_076	2.5992	38.34	4.27E-13	400	2.6612	1.04	41.3	6.46E-13	n/a	n/a	n/a

Table S3. A summary of the Brazilian disc parameters for as-collected and TT samples.

As-collected				Post-thermal treatment			
Sample	Density	Porosity	TT	Density	Mass Reduction	Porosity	UTS
	(g/cm^3)	(%)	(°C)	(g/cm^3)	(g)	(%)	(MPa)
HYA_0m_001_Br	2.4899	31.09	n/a	n/a	n/a	n/a	1.53
HYA_0m_002_Br	2.5139	33.67	n/a	n/a	n/a	n/a	1.21
HYA_0m_003_Br	2.4877	32.05	n/a	n/a	n/a	n/a	1.69
HYA_0m_004_Br	2.545	33.04	n/a	n/a	n/a	n/a	1.5
HYA_0m_005_Br	2.5824	32.28	130	2.6346	0.32	35.67	0.98
HYA_0m_006_Br	2.5626	36.44	130	2.6214	0.39	39.95	0.96
HYA_0m_007_Br	2.562	38.9	130	2.6166	0.42	42.4	0.92
HYA_0m_008_Br	2.5598	34.78	130	2.6157	0.36	38.41	1.07
HYA_0m_009_Br	2.5453	38.07	130	2.6059	0.39	41.69	0.79
HYA_0m_010_Br	2.5122	37.56	185	2.5993	0.47	42.36	0.97
HYA_0m_011_Br	2.6096	36.32	185	2.6402	0.33	38.99	0.82
HYA_0m_012_Br	2.52	41.33	185	2.6095	0.42	45.86	0.86
HYA_0m_013_Br	2.524	39.53	185	2.6098	0.49	43.86	0.91
HYA_0m_014_Br	2.4942	36.79	185	2.5956	0.59	42.22	1
HYA_0m_015_Br	2.5498	36.18	400	2.7235	0.76	44.47	0.7
HYA_0m_016_Br	2.568	39.51	400	2.6707	0.66	45.59	0.63
HYA_0m_017_Br	2.5964	35.17	400	2.707	0.66	41.5	0.68
HYA_0m_018_Br	2.518	40.18	400	2.6618	0.75	47.3	0.69
HYA_0m_019_Br	2.5002	36.55	400	2.6419	0.82	44.19	0.8
HYA_0m_020_Br	2.5171	39.02	600	2.6952	0.73	46.69	0.7
HYA_0m_021_Br	2.5885	35.91	600	2.776	0.79	40.97	0.66
HYA_0m_022_Br	2.5028	38.59	600	2.7167	0.98	48.32	0.57
HYA_0m_023_Br	2.5168	38.59	600	2.717	1.01	47.64	0.66
HYA_0m_024_Br	2.5295	35.99	600	2.7473	0.94	46.16	0.54

2. Clay-separated XRD

Clay separated XRD measurements were performed on as-collected, surficial hyaloclastite for unglycolated and glycolated samples. The d(060) peak is at 60.35°, whilst the d(001) peak transitions from 15 Å to 16.2 Å, upon glycolation. Raw X-ray diffractograms are presented in Figure SI1 a and b.

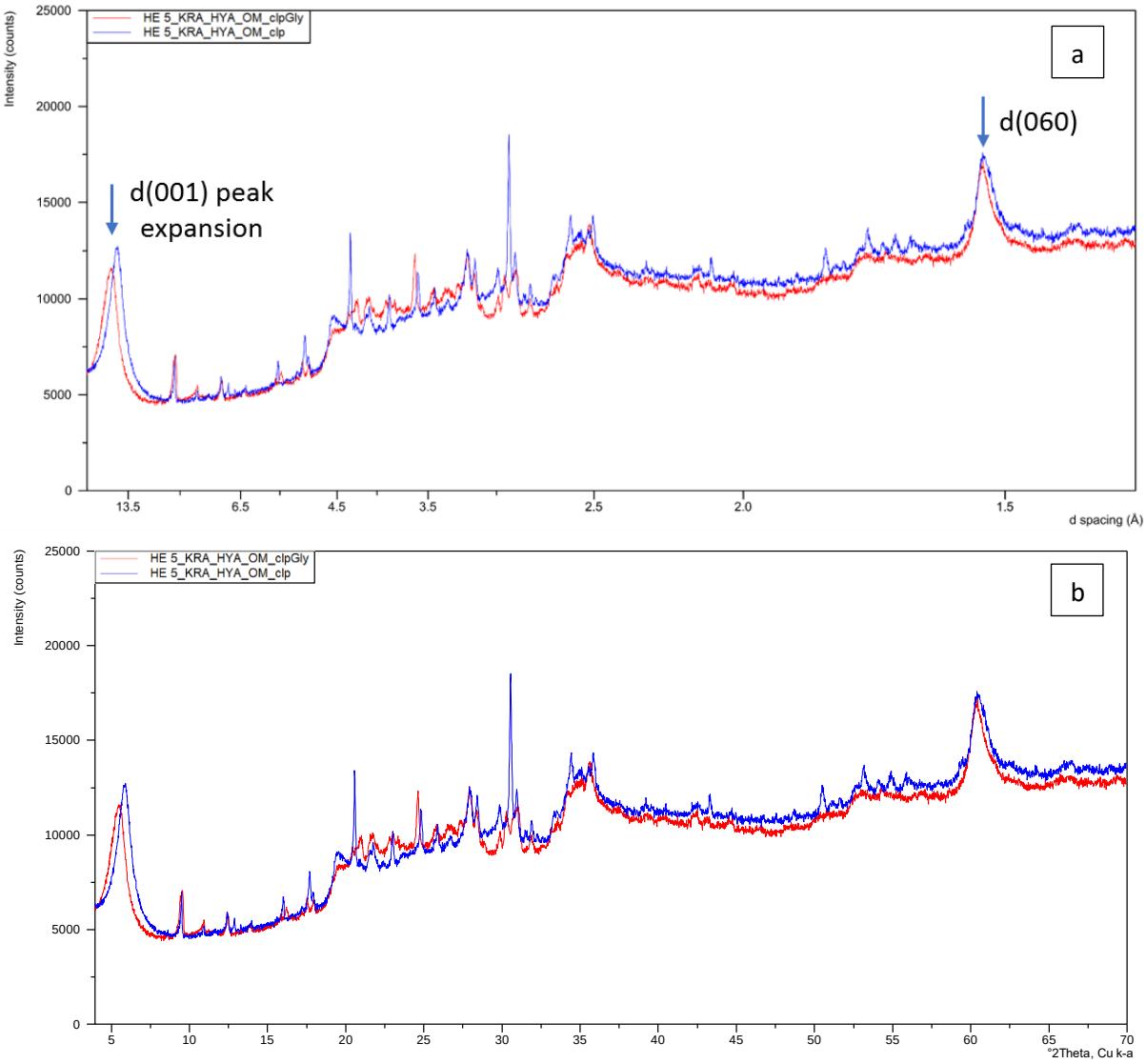

Figure S1. X-ray diffractograms of as-collected, gylcolated and unglycolated surficial hyaloclastite; **a.** intensity presented against °2Theta Cu k-a; **b**. intensity presented against angstroms.

3. QEMSCAN Images

We present here the full QEMSCAN images, acquired at 20 µm for as-collected (Fig. S2) and thermally treated (TT) samples (Fig. S3 – S6), that are used in the quantification of the mineral distribution (Table 2, main paper). Fig. S7 provides an annotated example of the various petrographic images presented in Figure 3 (main paper).

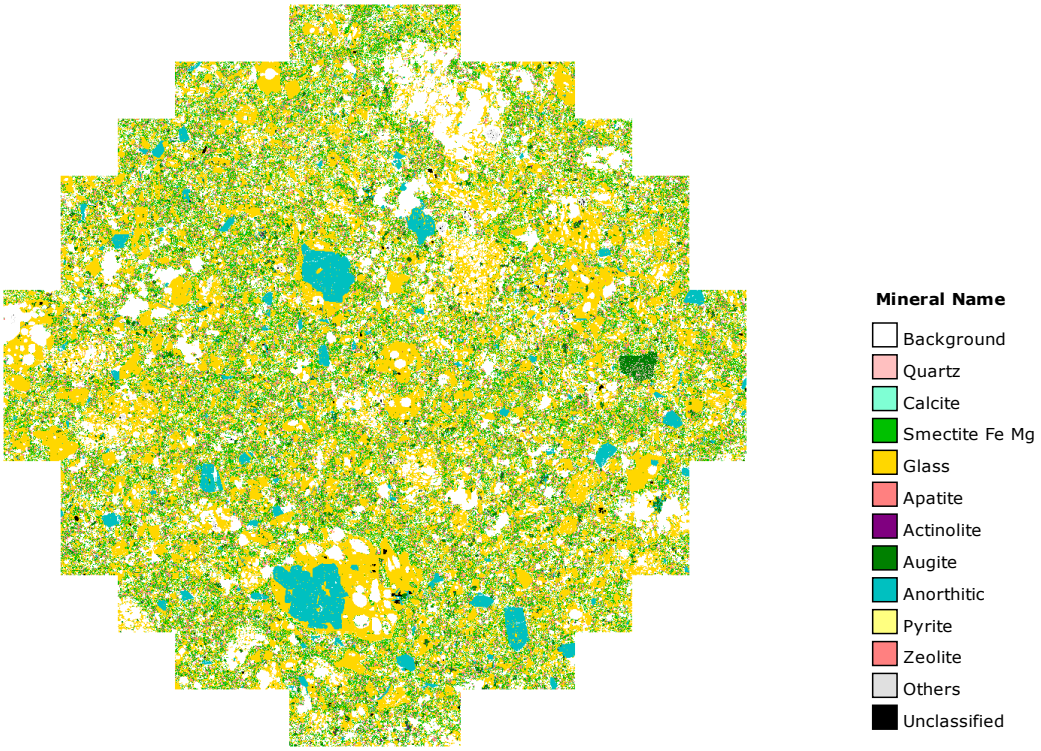

Figure S2. Mineral distribution of as-collected hyaloclastite, acquired using QEMSCAN at 20 µm resolution.

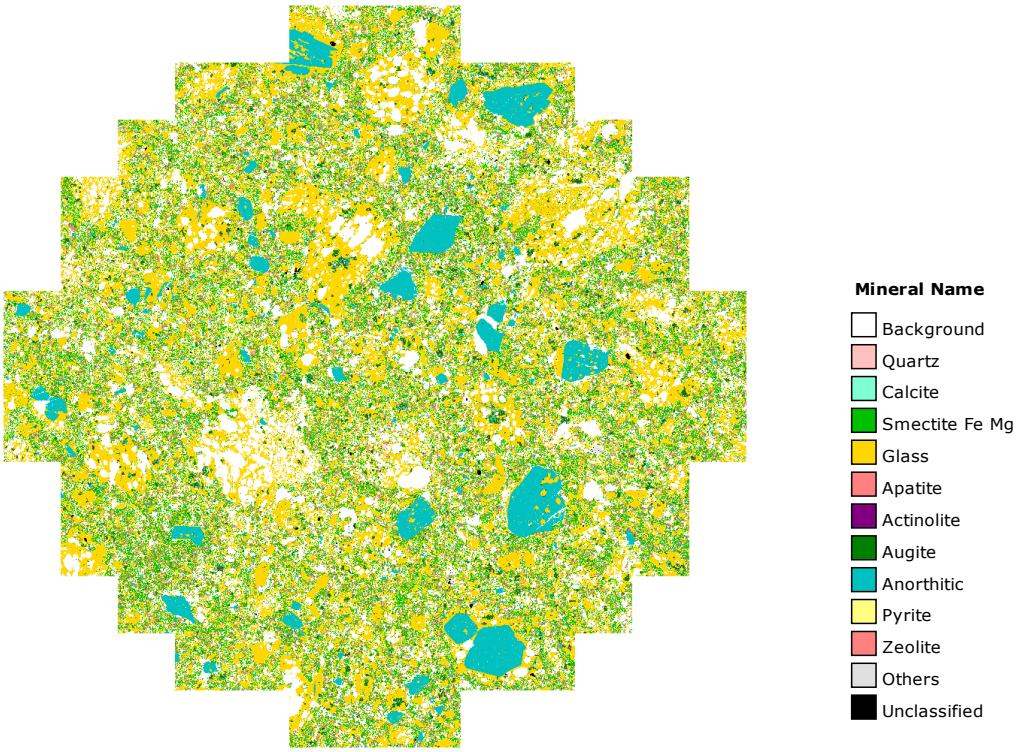

Figure S3. Mineral distribution of hyaloclastite, TT to 130°C for 12 hours, and acquired using QEMSCAN at 20 µm resolution.

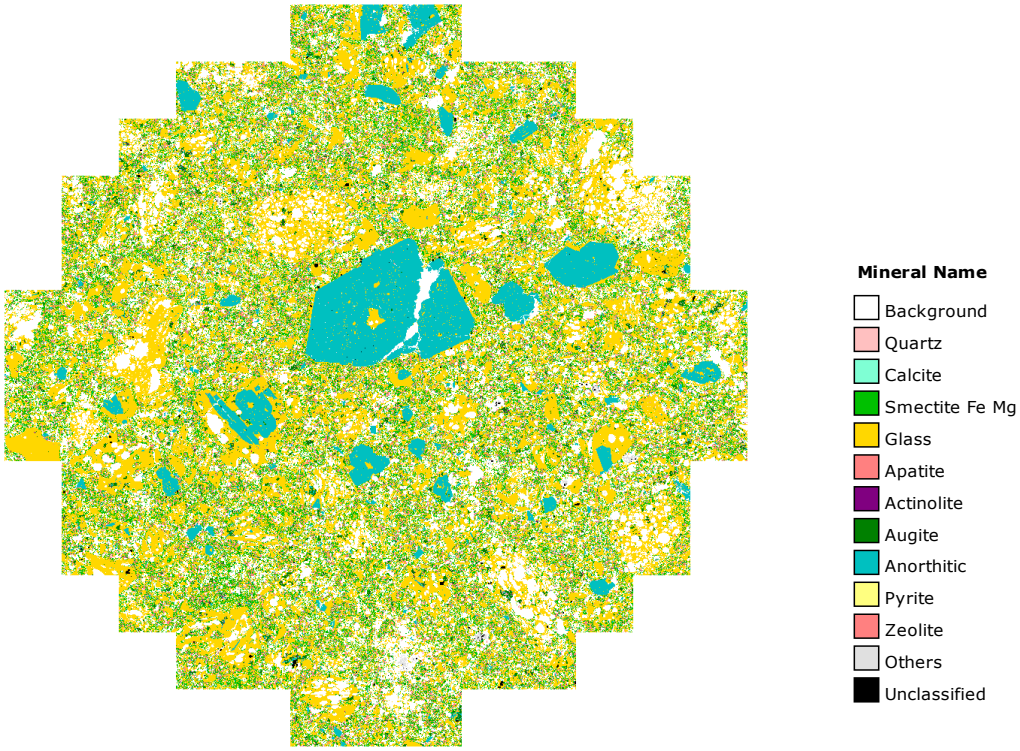

Figure S4. Mineral distribution of hyaloclastite, TT to 185°C for 12 hours, and acquired using QEMSCAN at 20 µm resolution.

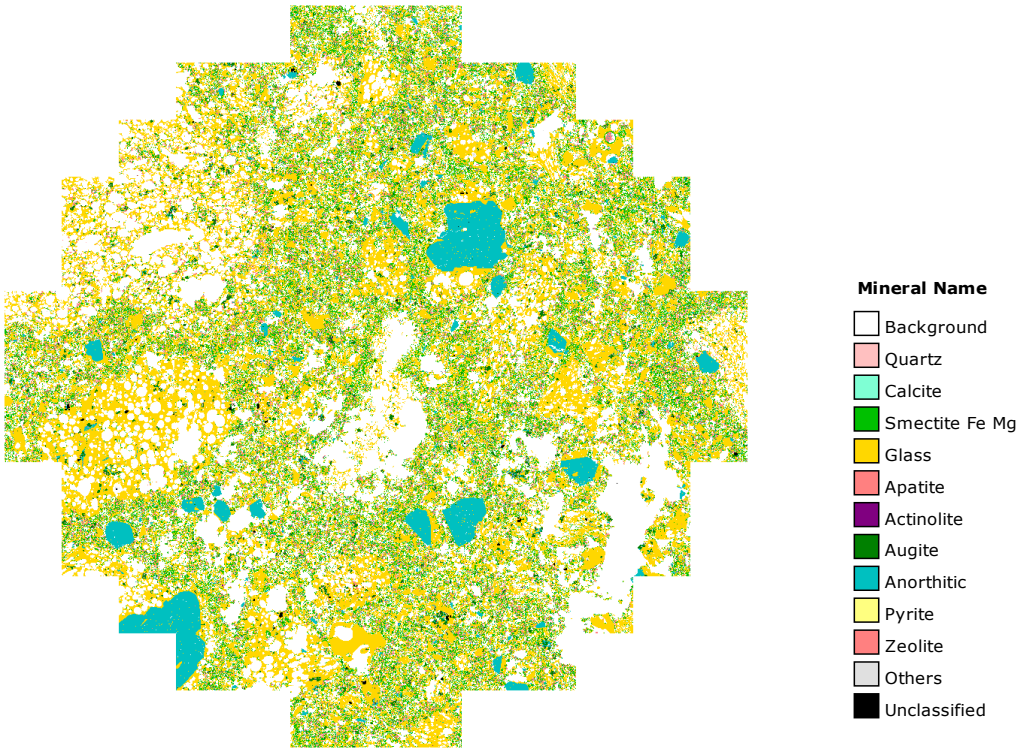

Figure S5. Mineral distribution of hyaloclastite, TT to 400°C for 12 hours, and acquired using QEMSCAN at 20 µm resolution.

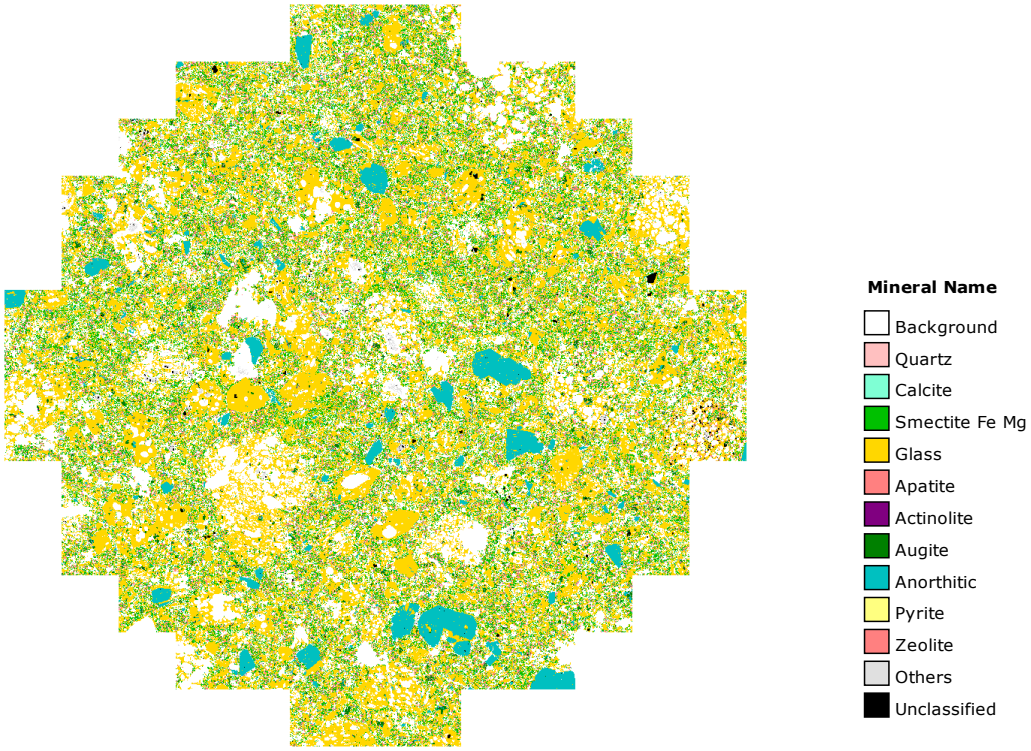

Figure S6. Mineral distribution of hyaloclastite, TT to 600°C for 12 hours, and acquired using QEMSCAN at 20 µm resolution.

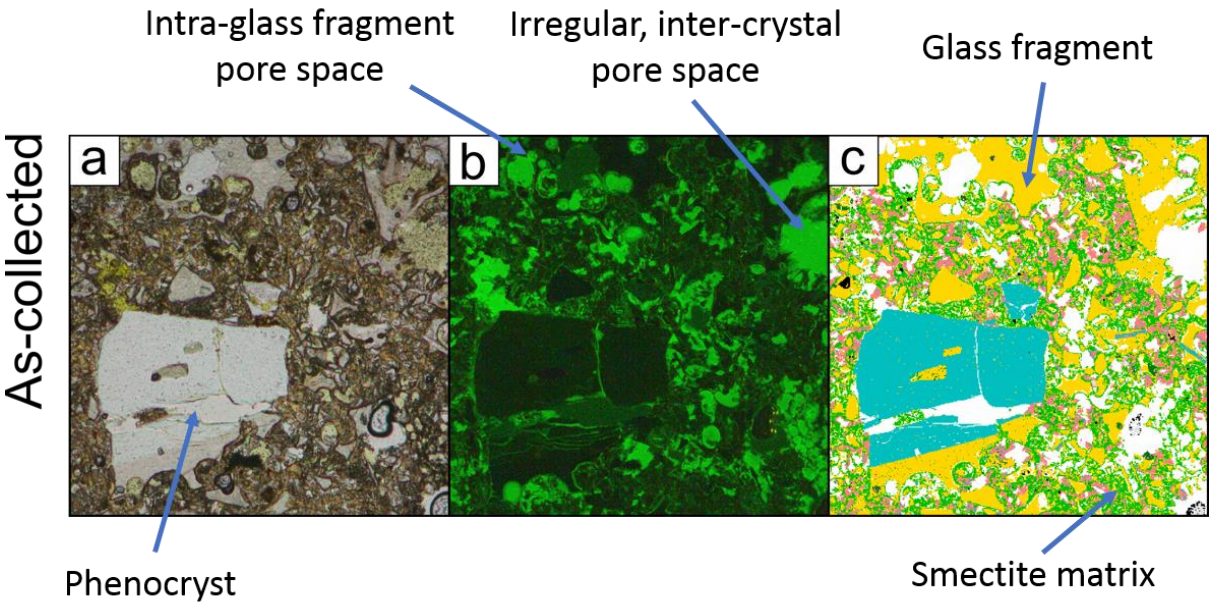

Figure S7. Annotated example from Figure 3 (main paper). a. Plain polarised light image from an optical microscope; b. Ultraviolet pore space map using florescent dyed thin section; c. QEMSCAN image showing mineral distribution

4. Additional Strength Curves

Figure 6c in the main paper presents a subset of the total tensile strength dataset, for easier viewing. Here, we present the other strength curves not shown in the main paper (Fig. S8).

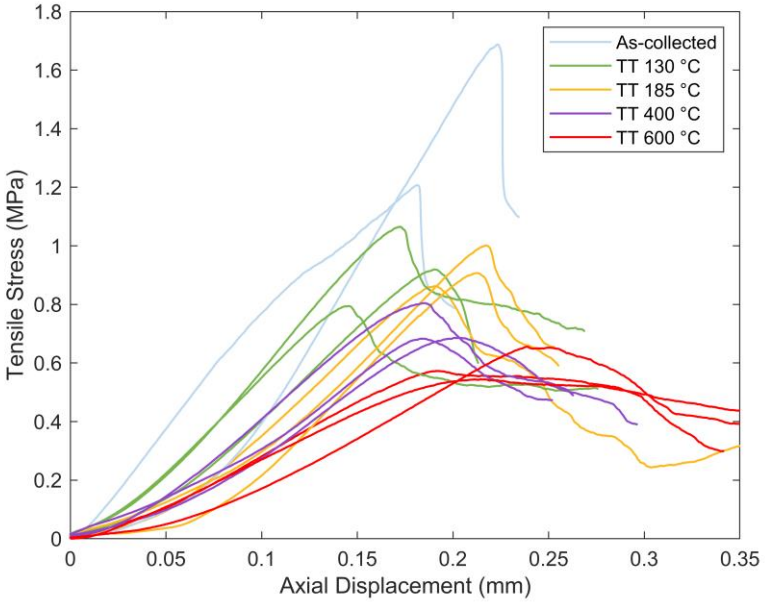

Figure S8. Additional tensile strength curves for as-collected and TT surficial material.